Transactions, SMiRT-22
San Francisco, California, USA - August 18-23, 2013
Division V

SEISMIC ISOLATION WITH TWO-DIMENSIONAL PERIODIC FOUNDATIONS

Y.Q. Yan[1], Z.B. Cheng[2], Farn-Yuh Menq[3], Y.L. Mo[4], Z.F. Shi[5] and Kenneth H. Stokoe, II[6]

[1] PhD student, Dept. of Civil Engineering, University of Houston, Houston, TX
[2] PhD student, School of Civil Engineering, Beijing Jiaotong University, Beijing, China
[3] Operations Manager, NEES-UTEXAS, University of Texas, Austin, TX
[4] Prof., Dept. of Civil Engineering, University of Houston, Houston, TX (yilungmo@central.uh.edu)
[5] Prof., School of Civil Engineering, Beijing Jiaotong University, Beijing, China
[6] Graves Chair Prof., Dept. of Civil, Architectural and Env. Engineering, University of Texas, Austin, TX

ABSTRACT

Foundations were designed using two-dimensional (2D) periodic materials for seismic isolation. Theories of the 2D periodic foundation are presented. Numerical analyses of the 2D periodic foundations were conducted to determine the frequency bands in which stress waves cannot propagate through the periodic foundations. These frequency bands are called the band gaps. These band gaps are then verified with 3D FEM models by scanning frequency analysis. Field experiments of a scaled specimen were conducted to validate the numerical and finite element analysis. Test results show the 2D periodic foundation can effectively reduce the response of the upper structure for excitations within the frequency band gaps. Test results agree with the finite element analysis, and indicate that 2D periodic foundation is a feasible way in reducing seismic vibrations.

1. INTRODUCTION

Advanced fast nuclear power plants (AFR) and small modular fast reactors (SMFR) are composed of thin–walled structures such as pipes. For this type of structures, seismic isolation is an effective solution for mitigating earthquake hazards. In conventional isolators such as high damping rubber bearings, lead-rubber bearings, and friction pendulum bearings, large relative displacements occur between upper structures and foundations. Recently Thomas et al. (2006) introduced the mechanism of periodic materials, which provides a new approach for vibration isolation. Xiang and Shi (2009) conducted numerical study on flexural vibration periodic beams, and through comprehensive parametric studies, the existence of vibration gaps is found. Based on the theory of elastodynamics, a feasibility study on layered periodic foundations is reported (Xiang et al. 2010). The layered periodic foundation with two different materials, rubber and concrete, have frequency band gaps within 20Hz. Periodic foundations have unique dynamic properties to block stress waves in certain frequencies. As a result, the periodic foundation isolates motions falling in the frequency band gaps. Both theoretical and experimental studies have been conducted to investigate the layered periodic foundations (Xiang et al. 2012).

In this paper, the basic theory of two-dimensional (2D) periodic foundations is presented, and finite element models for 2D periodic foundations with an upper structure are set up in order to determine the frequency band gaps, which are obtained by scanning frequency analysis, to resist seismic loading. The experimental program is presented and the test results are analyzed and compared to the finite element analysis results. It is observed that when the main exciting frequency falls within the frequency band gaps, the response of the structure on a 2D periodic foundation is significantly reduced when compared to the one without a 2D periodic foundation.

2. THEORETICAL BACKGROUND AND SOLUTION

Consider a particle in an isotropic linear elastic solid of infinite extension. In the absence of external forces, and omitting damping, the governing equations in XY plane of vibration for continuum (Kushwaha et al. 1994), are

$$(\lambda+2\mu)\frac{\partial^2 u}{\partial x^2}+\mu\frac{\partial^2 u}{\partial y^2}+(\lambda+\mu)\frac{\partial^2 v}{\partial x\partial y}=\rho\frac{\partial^2 u}{\partial t^2} \tag{1}$$

$$(\lambda+2\mu)\frac{\partial^2 v}{\partial y^2}+\mu\frac{\partial^2 v}{\partial x^2}+(\lambda+\mu)\frac{\partial^2 u}{\partial x\partial y}=\rho\frac{\partial^2 v}{\partial t^2} \tag{2}$$

Where u and v are displacements in the X and Y directions, respectively; ρ is the material density; λ, and μ are the Lame constants. Eqs. (1) and (2) are derived from the phononic crystal theory.

To solve the governing equations, the Plane Wave Expansion (PWE) method was used. According to the Bloch theorem (Kushwaha et al. 1994), the material constants in Eqs. (1) and (2) may all be expanded in a Fourier series. Together with the periodic boundary conditions, as well as taking into account the stress and strain relationships (Landau and Lifshitz 1986), one can obtain the characteristic equations for the XY mode of periodic structures, i.e. Eqs. (3) and (4) (Wen et al. 2009):

$$\begin{aligned}
&\omega^2\sum_{\mathbf{G}'}\rho(\mathbf{G}''-\mathbf{G}')u_{\mathbf{k}+\mathbf{G}'}\\
&=\sum_{\mathbf{G}'}\Big[\alpha(\mathbf{G}''-\mathbf{G}')(\mathbf{k}+\mathbf{G}')_x(\mathbf{k}+\mathbf{G}'')_x+\mu(\mathbf{G}''-\mathbf{G}')(\mathbf{k}+\mathbf{G}')_y(\mathbf{k}+\mathbf{G}'')_y\Big]u_{\mathbf{k}+\mathbf{G}'}\\
&+\sum_{\mathbf{G}'}\Big[\beta(\mathbf{G}''-\mathbf{G}')(\mathbf{k}+\mathbf{G}')_y(\mathbf{k}+\mathbf{G}'')_x+\mu(\mathbf{G}''-\mathbf{G}')(\mathbf{k}+\mathbf{G}')_x(\mathbf{k}+\mathbf{G}'')_y\Big]v_{\mathbf{k}+\mathbf{G}'}
\end{aligned} \tag{3}$$

$$\begin{aligned}
&\omega^2\sum_{\mathbf{G}'}\rho(\mathbf{G}''-\mathbf{G}')v_{\mathbf{k}+\mathbf{G}'}\\
&=\sum_{\mathbf{G}'}\Big[\beta(\mathbf{G}''-\mathbf{G}')(\mathbf{k}+\mathbf{G}')_x(\mathbf{k}+\mathbf{G}'')_y+\mu(\mathbf{G}''-\mathbf{G}')(\mathbf{k}+\mathbf{G}')_y(\mathbf{k}+\mathbf{G}'')_x\Big]u_{\mathbf{k}+\mathbf{G}'}\\
&+\sum_{\mathbf{G}'}\Big[\alpha(\mathbf{G}''-\mathbf{G}')(\mathbf{k}+\mathbf{G}')_y(\mathbf{k}+\mathbf{G}'')_y+\mu(\mathbf{G}''-\mathbf{G}')(\mathbf{k}+\mathbf{G}')_x(\mathbf{k}+\mathbf{G}'')_x\Big]v_{\mathbf{k}+\mathbf{G}'}
\end{aligned} \tag{4}$$

Where $\mathbf{G''}=\mathbf{G}+\mathbf{G'}$, $\alpha=2\mu(4\lambda+\mu)/(2\lambda+\mu)$, and $\beta=4\lambda\mu/(2\lambda+\mu)$. If the wave vector $\mathbf{k}$ is given in the First *Brillouin* zone and $\mathbf{G}$ is taken points in the reciprocal space, then a set of eigenvectors $u_{\mathbf{k}+\mathbf{G}'}$ and eigenvalues ω can be obtained. In other words, to get the dispersion curve, selecting wave vector $\mathbf{k}$ in the First *Brillouin* zone with three vertices Γ, X and M, a series of ω can be obtained (Kushwaha et al. 1994).

Figure 1 shows the relationship between the wave vector $\mathbf{k}$ and eigenvalues ω of the 2D periodic foundation with the geometric and material properties in Section 3.1. The wave vector travelling through three vertices Γ, X and M of the First *Brillouin* zone as shown in the horizontal axis in Figure 1 and the corresponding ω are shown in the vertical axis in Figure 1 . The frequency band in yellow, 40Hz - 60Hz, is shown as the frequency band gap, which means the propagation of the wave is blocked.

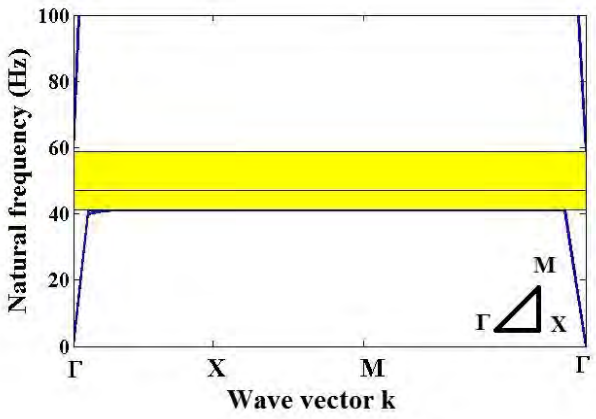

Figure 1. Attenuation zones

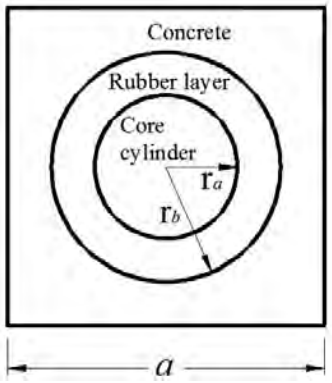

Figure 2. One unit cell

3. FINITE ELEMENT ANALYSIS

3.1 Geometric and Material Properties

Many variables may affect the frequency band gaps and their widths of the 2D periodic foundation. In order to obtain the lower frequency band gap and wider band width, the finite element model of one unit cell, shown in Figure 2, was set up to conduct the parametric analysis. The results are summarized below.

1) With the increase of core cylinder density, the starting frequency of the first band gap is lower.
2) If the Young's modulus of the rubber is small, the starting frequency of the first band gap is low.
3) With the increase of the filling ratio, the starting frequency of the first band gap will decrease.
4) When the ratio of the radius of the core cylinder to the thickness of rubber layer equals 1.5, the starting frequency of the first band gap reaches its minimum value.

Therefore, the following geometric properties and the material properties are used in the finite element analysis and the following experimental program. The geometric properties of the test specimens are listed in Table 1. The material properties are shown in Table 2.

Table 1: Geometric properties for one unit cell

Part	Material	Dimension
Core cylinder	Ductile cast iron	Diameter = 0.12 m.
Rubber coating	Supper soft rubber (Duro 10)	Outer diameter = 0.2 m.
Matrix	Reinforced Concrete	Length of unit cell (a) = 0.254 m

Table 2: Material properties

Material	Density (kg/m^3)	Young's Modulus (Pa)	Poisson's ratio
Ductile cast iron	7.184×10^3	1.65×10^{11}	0.275
Supper soft rubber	1.196×10^3	5.7×10^5	0.463
Steel	7.85×10^3	2.05×10^{11}	0.28
Concrete	2.3×10^3	3.144×10^{10}	0.33

3.2 Simulation and Results

An ABAQUS model was set up to get the dynamic characteristics of the specimen. The dimension of the frame and the additional mass assigned on the top of the frame are the same as those used in the test specimen, and are detailed in Section 3.1. The material properties, which are the same as the test specimen, are also illustrated in Section 3.1.

For the ABAQUS model, the displacements of the bottom surface in Y and Z directions were fixed, and an instantaneous displacement in the X-direction with an amplitude δ_i was applied at the bottom, as shown in Figure 3. These boundary conditions simulate the input motion of the horizontal component of harmonic motion or an earthquake. The displacement in the X direction of node A at the top of the frame is denoted by δ_o. To assess the efficiency of the periodic foundation in the frequency domain, a Frequency Response Function (FRF) is defined as 20 $\log(\delta_o/\delta_i)$. When the output δ_o is equal to the input δ_i, the value of FRF equals zero. When the output displacement is 31.6% of the input displacement, the value of FRF is -10, which means the periodic foundation significantly reduces the propagation of waves. As shown in Figure 4, the ranges of attenuation zone are 40Hz-42.5Hz, 43Hz-84.5Hz, 86Hz-100Hz. Theoretically, when the input waves fall in the band gaps, the response of the frame can be reduced significantly compared to the frame response without the periodic foundation.

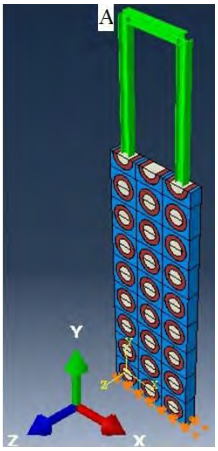

Figure 3. Boundary conditions under shear-mode waves

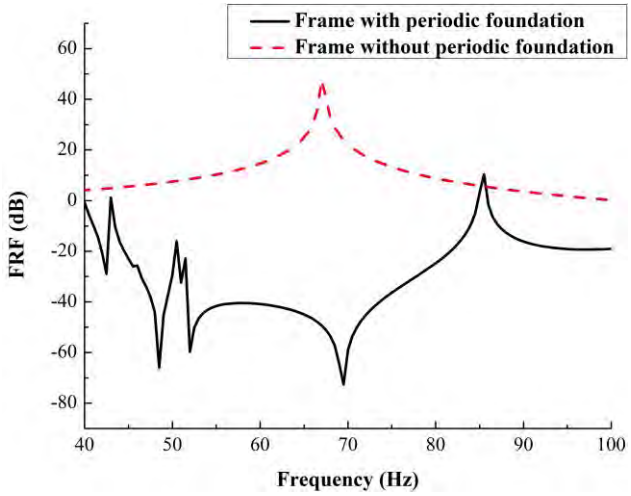

Figure 4. Frequency Response Function (FRF) of node A

4. EXPERIMENTAL PROGRAM

4.1 Test Setup and procedures

Two specimens were tested. Figure 5 shows the test setup of the two specimens. The dimension and the material properties are shown in Section 3.1, Table 1 and Table 2 respectively. The reinforced concrete foundation with an upper steel frame is shown as Specimen C and the periodic foundation with an upper steel frame is shown as Specimen D in Figure 5. Three-dimensional accelerometers were used to measure the acceleration in the X directions, see Figure 5. The accelerometers were arranged on the top of the steel frame and on the top of the concrete footings of both specimens.

The input seismic motions were provided by a tri-axial shaker at the University of Texas at Austin named T-Rex (http://nees.utexas.edu). T-Rex is capable of shaking in three directions as: vertical, horizontal in-line and horizontal cross line. For this test, horizontal in-line was used to generate horizontal vibration along the X direction shown in Figure 5.

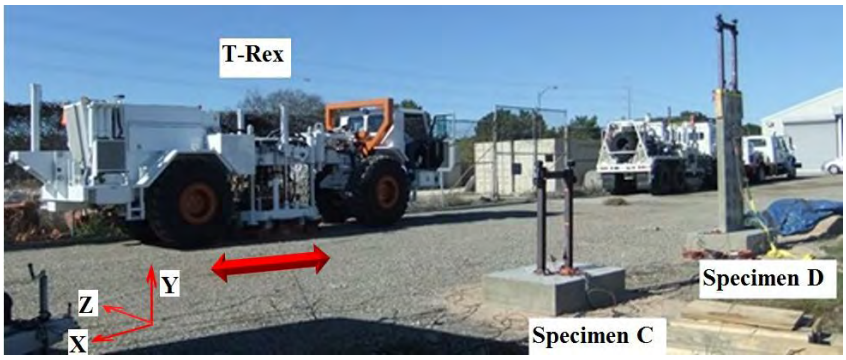

Figure 5. Picture of field test setup

Three different types of tests are conducted. Stepped-sine tests were first conducted to determine the frequency band gaps of the periodic foundation. A stepped sine test is a test function provided by the Data Physics SignalCal 730 dynamic signal analyzer. It is comparable to the scanning frequency analysis in FEM analyses. Fixed frequency sine waves from 100 Hz down to 40 Hz were applied to the test specimens according to the numerical analysis results in Section 3.2. Amplitudes and phases of each sensor at each frequency step were recorded. Based on stepped-sine test results, harmonic excitations with a fixed frequency were applied to the specimens. In the last step, seismogram obtained from the Pacific Earthquake Engineering Research (PEER) Ground Database was used as the input motion for the seismic tests. In the last two tests, time histories of each sensor were recorded.

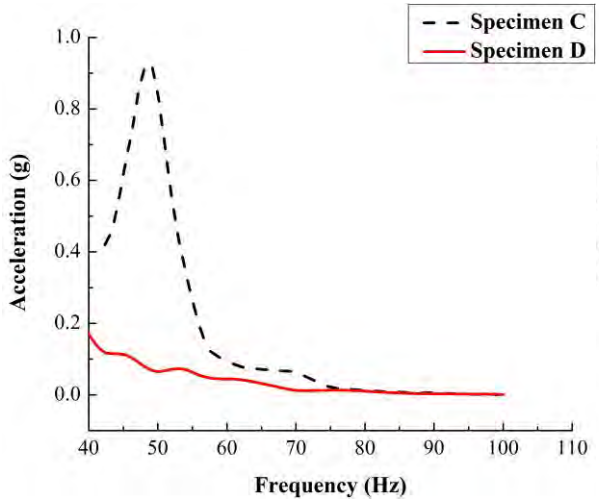

Figure 6. Accelerations at the top of both Specimens C and D

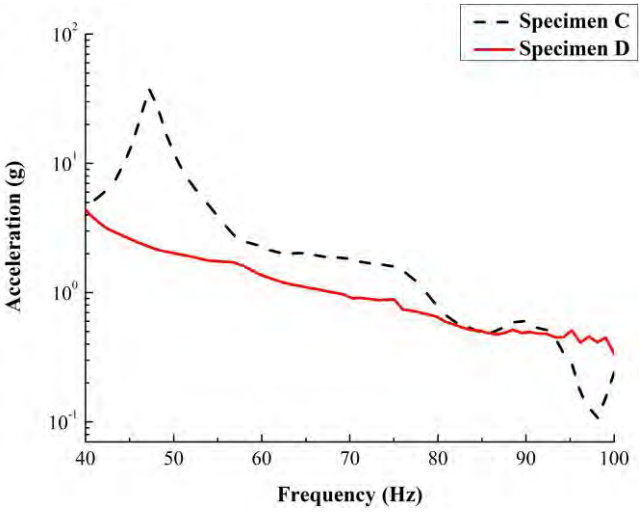

Figure 7. Transfer function for both Specimens C and D

4.2 Stepped Sine Tests and Results

Figure 6 shows the acceleration in X direction measured on top of the two steel frames from the stepped sine tests. As shown in the figure, steel frame on Specimen C experienced a higher level of acceleration at most frequencies, and especially at 50Hz. Although not shown here, both foundations were subjected to similar level of shaking. To eliminate possible differences of shaking levels between the two foundations, the acceleration on top of the steel frame were normalized by the acceleration measured on

the foundations. Figure 7 shows the amplitudes of the transfer functions from both specimens. The transfer function is the ratio between the acceleration measured on the top of the frame to that measured on the concrete foundation. When the amplitudes of the transfer functions of Specimen D are less than those of Specimen C, seismic motions are isolated by the periodic foundation. As shown in Figure 7, band gaps are in the frequency ranges of 40Hz-84Hz and 86Hz-93Hz. To better illustrate the test results, the ratio of transfer function from Specimen D to the transfer function from Specimen C are ploted in Figure 8. Band gaps are where the ratio is smaller than 1 (below the black dash line shown in Figure 8).

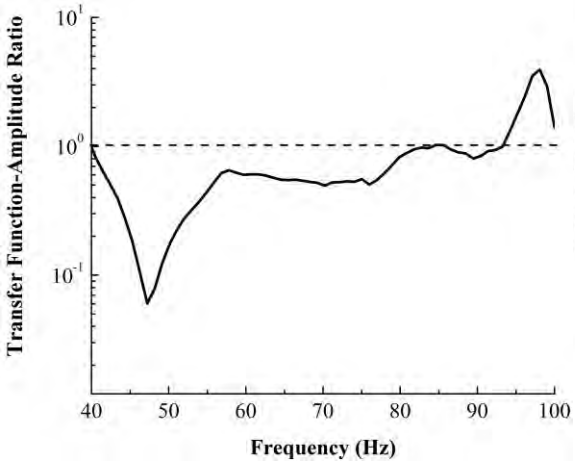

Figure 8. Ratio of transfer function

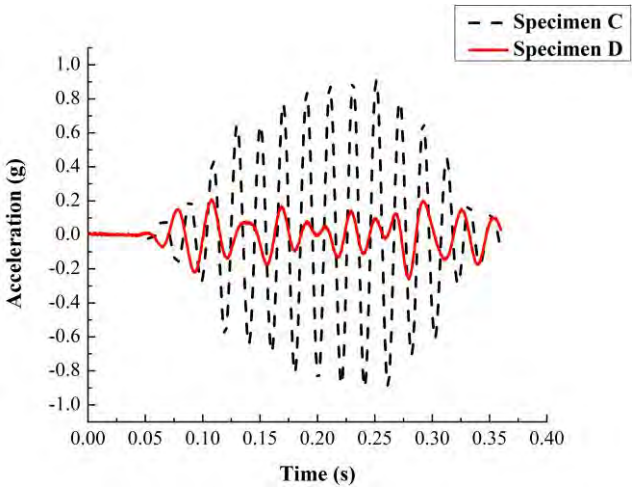

Figure 9. Acceleration in X direction on the top of the frame under a sine wave of 50Hz

4.3 Fixed Sine Tests and Results

From the stepped sine tests, the frequency band gaps of the periodic foundation with a steel frame are found to be 40Hz-84Hz and 86Hz-93Hz. To verify the effect of the frequency band gaps, a single frequency sinusoid wave was applied to the specimens within the range of the band gaps, i.e. 50Hz. Figure 9 shows the accelerations in the X direction on the top of the frame under a sine wave with a frequency of 50Hz. The dashed black curve is the acceleration response on top of the steel frame on a concrete foundation (i.e., Specimen C); while the red curve is the acceleration at the top of the frame on a periodic foundation (i.e., Specimen D). It can be seen that for the frame on the periodic foundation, the peak acceleration is reduced to 25% of the peak acceleration on the frame without the periodic foundation.

4.4 Seismic Tests and Results

Modified seismograms were used to verify the frequency band gap effects. To find the main frequency of each seismic record, Fourier transformations were used in determining the corresponding frequency spectrum. The frequency at which the amplitude reaches its maximum value is considered as the main frequency. Two seismic records from the PEER Ground Database were used in the field tests, i.e. Bishop (Rnd Val) P0486/MCG-UP (1984/11/23) with the main frequency of 8.3Hz and Bishop (Rnd Val) P0486/MCG-360 (1984/11/23) with the main frequency of 8.16Hz. Both seismic records were modified to make the main frequency match the band gaps, i. e. 50Hz. Figures 10 and 11 show the modified seismogram of Bishop (Rnd Val) P0486/MCG-UP (1984/11/23) with frequency of 50Hz in time and

frequency domains, respectively. Additionally, the modified seismogram of Bishop (Rnd Val) P0486/MCG-360 (1984/11/23) in both time and frequency domains are shown in Figures 12 and 13.

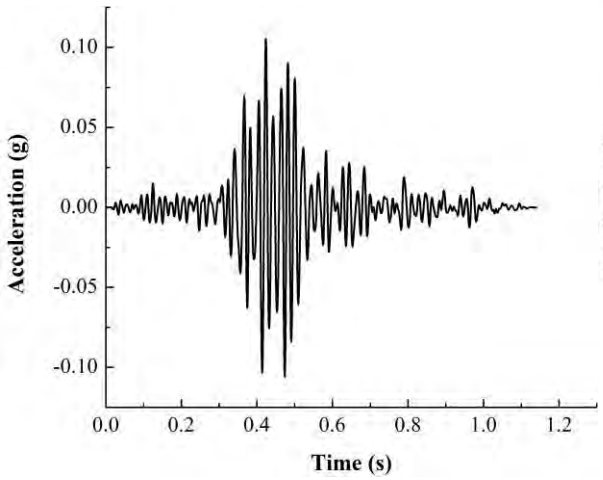

Figure 10. Modified Bishop P0486-UP in time domain

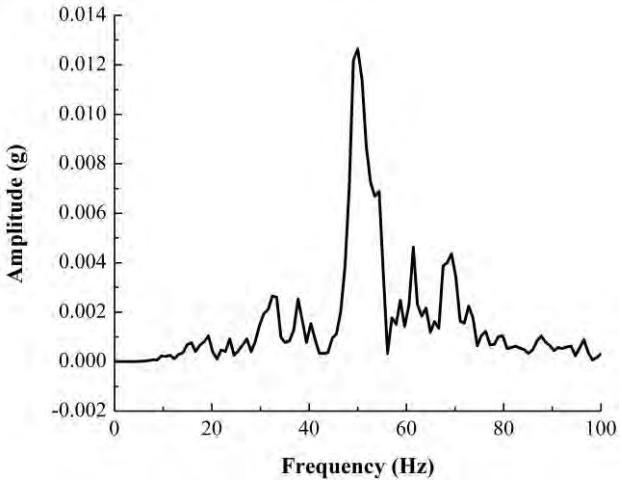

Figure 11. Modified Bishop P0486-UP in frequency domain

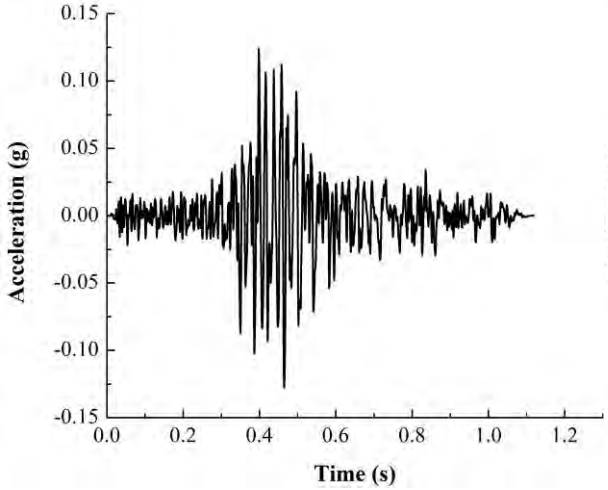

Figure 12. Modified Bishop P0486-360 in time domain

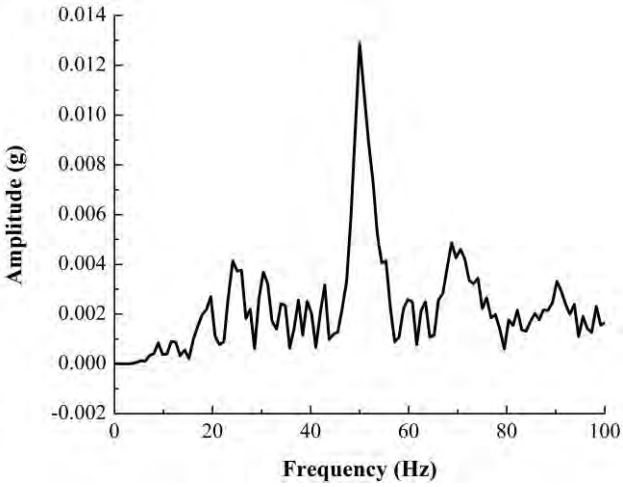

Figure 13. Modified Bishop P0486-360 in frequency domain

The horizontal acceleration time histories under the excitation of the modified Bishop (Rnd Val) P0486/MCG-UP (1984/11/23) on top of the steel frames from both specimens are shown in Figure 14. It is found that for the frame on the periodic foundation (i.e., Specimen D), the peak acceleration in the X direction is reduced by as much as 60%, when compared to that of the frame without the periodic foundation (i.e., Specimen C). The responses of the two specimens under the modified seismogram Bishop (Rnd Val) P0486/MCG-360 (1984/11/23) are shown in Figure 15. The peak acceleration on the top of the frame was reduced by 30%, as compared to the specimen without the periodic foundation. The reductions shown in Figure 15 is less than those shown in Figure 14. This is caused by the frequency contents of the input motions. Although the main frequency of the two input motions are at 50Hz the input motions shown in Figure 13 has energy in frequency ranges fall outside of the band gaps.

Overall, the test results indicate that the periodic foundation is capable of providing effective isolations for the vibrations fall into the designed band gap.

4.5 Comparison of Experimental Results with Analytical Outcomes

The results from the fixed sine tests and the seismic tests show that the periodic foundation can reduce the response of the steel frame significantly when the exciting S-wave frequencies fall into the band gaps. The stepped sine wave test shows that when the exciting frequencies are between 40Hz-84Hz and 86Hz-93Hz, shown in Figures 6 to 8, the acceleration on the top of the frame was reduced due to the periodic foundation. The analytical results in Section 3 show the band gaps of the periodic foundation are in the ranges of 40Hz-42.5Hz, 43Hz-84.5Hz, and 86Hz-100Hz, as seen in Figure 4. The experimental results agree fairly well with the finite element analysis.

From the finite element analysis, the band gaps of the periodic foundation fall within the fundamental frequency of the upper steel frame, which will avoid resonance at the fundamental frequency. The harmonic tests show that the periodic foundation can block the S-wave in specified frequency. Therefore, the band gaps of the periodic foundation can be designed to match the fundamental frequency of the upper structure.

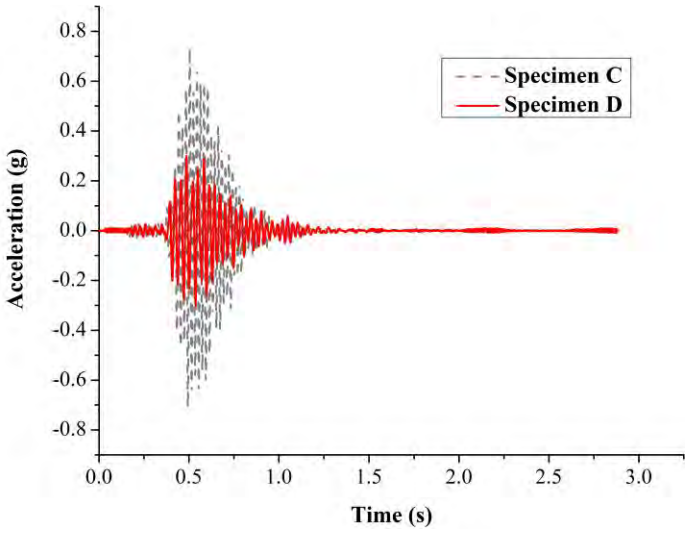

Figure 14. Acceleration in X direction on the top of the frame under modified Bishop (Rnd Val) P0486/MCG-UP (1984/11/23) with the main frequency of 50Hz

5. CONCLUSIONS

In the field tests performed, the accelerations of the specimens were recorded and analyzed to find the frequency band gaps, and to verify the frequency band gap effects of the periodic foundation. The accelerations on the top of the frame with and without the periodic foundation were compared. According to the test results, the periodic foundation can filter out S-waves with frequencies falling into the band gaps. The acceleration at the top of the frame on the periodic foundation can be reduced by as much as 75%. Moreover, the results of the stepped sine S-wave are consistent with those obtained from the finite element analysis. Theoretical and experimental results confirm the significant vibration attenuation when the exciting frequency falls into the band gaps.

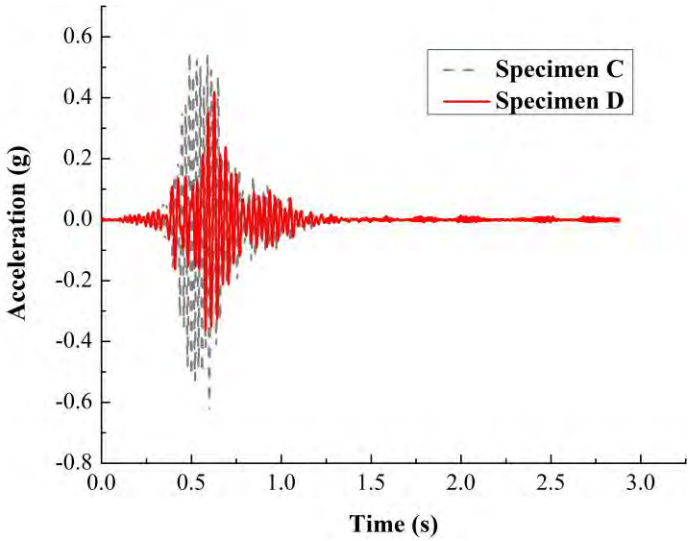

Figure 15. Acceleration in X direction on the top of the frame under modified Bishop (Rnd Val) P0486/MCG-360 (1984/11/23) with the main frequency of 50Hz

6. ACKNOWLEDGEMENTS

This work is supported by the US Department of Energy NEUP program (Proj. No. 3219) and the National Natural Science Foundation of China (51178036). The opinions expressed in this study are those of the authors and do not necessarily reflect the views of the sponsors.

7. REFERENCES

Kushwaha, M.S., Halevi, P., Martnez, G.,Dobrzynski, L.,Djafari-Rouhani, B. (1994). "Theory of Acoustic Band Structure of Periodic Elastic Composites," *Physics Review B*, 49 (4), 2313-2322.

Landau, L.D., Lifshitz, E.M. (1986). *Theory of Elasticity (3rd edition)*. New York: Pergamon Press, 13-15.

PEER (2011) Peer Ground Motion Database, http://peer.berkeley.edu/peer_ground_motion_database.

Thomas, E.L., Gorishnyy, T. and Maldovan, M. (2006). "Phononics: Colloidal Crystals Go Hypersonic," *Nature Materials* 5, 773 – 774.

Wen, X. S., Wen, J. H., Yu, D.L., Wang, G., Liu, Y. Z., Han, X. Y., (2009). *Phononic Crystals*. National Defense Industry Press. 245-247. (in Chinese)

Xiang, H. J., Shi, Z. F. (2009). "Analysis of Flexural Vibration Band Gaps in Periodic Beams Using Differential Quadrature Method," *Computers and Structures*, 87(23-24), 1559-1566.

Xiang, H. J., Shi, Z. F., Bao, J. (2010). "Seismic Isolation of Buildings With A New Type of Periodic Foundations," *Earth and Space 2010: Engineering, Science, Construction, and Operations in Challenging Environments*, ASCE, Honolulu, HA, 2992-3001.

Xiang, H.J., Shi, Z.F., Wang, S.J. and Mo, Y.L. (2012). "Periodic Materials-based Vibration Attenuation in Layered Foundations: Experimental Validation," *Smart Materials and Structures*, 21(11), 112003-112012.